

## PRE-FORMULATION STUDY ON 5-FLUOROURACIL AND CERTAIN LIPIDS FOR SOLID LIPID NANOPARTICLES PREPARATION

MONA M. ELKHATIB<sup>1\*</sup>, AMIR I. ALI<sup>2</sup>, SUZAN A. ABDELRAZEK<sup>3</sup>, ALI S. AL-BADRAWY<sup>4</sup>

<sup>1</sup>Department of Pharmaceutics and Industrial Pharmacy, Faculty of Pharmacy, Cairo University, Cairo 11562, Egypt, <sup>2,3,4</sup>Military Medical Academy, Cairo 11774, Egypt

\*Email: elkhatibmona55@yahoo.com

Received: 30 Oct 2021, Revised and Accepted: 13 Dec 2021

### ABSTRACT

**Objective:** The study's objective involved compatibility studies to investigate the possible interactions between 5-fluorouracil (5-FU) and four different lipids, and the most appropriate lipid was chosen.

Differential scanning calorimetry (DSC), X-ray diffraction (XRD), and Fourier Transform Infrared spectroscopy (FT-IR) are used for the compatibility study between 5-FU and several excipients as cholesterol, Compritol®, stearic acid, and glycerol monostearate (GMS).

**Methods:** The physical mixture between 5-FU and each lipid was made by mixing of a certain amount of drug with the same amount of lipid. Drug lipid blended mixtures were made by solvent evaporation casting method. 5-FU alone, physical mixture and blended mixture were measured using Differential scanning calorimetry (DSC) to investigate melting peak of drug and effect of each lipid on this melting point, X-ray diffraction (XRD) to observe the crystalline or amorphous state of drug and Fourier Transform Infrared (FT-IR) to determine any chemical interaction between drug and these lipids by observing any shift happened to characteristic peaks related to the drug.

**Results:** 5-FU T<sub>m</sub> (280.04 °C) peak appeared in drug-lipid physical mixtures with minor changes in position while this peak disappeared in 5-FU-Compritol® and 5-FU-cholesterol blended mixture, indicating that the drug is molecularly dispersed. XRD result showed that the crystalline structure of 5-FU was present in physical mixtures with four lipids, while in the 5-FU-Compritol® blended mixture, the crystalline state of the drug was disappeared, confirming the DSC result.

The FT-IR spectrum of the 5-FU-physical mixtures with four lipids showed that all characteristic peaks of the drug appeared with minor changes. In the case of 5-FU-blended mixtures with mentioned lipids, no chemical interaction occurred between the drug and mentioned lipids except in the drug-stearic acid blended mixture, the N-H peak at 3136.25 cm<sup>-1</sup> was disappeared due to amide ester formation.

**Conclusion:** The most appropriate lipids suitable for the preparation of 5-FU solid lipid nanoparticles were GMS and cholesterol.

**Keywords:** 5-fluorouracil, Glycerol monostearate, Stearic acid, Compritol®, Cholesterol

© 2022 The Authors. Published by Innovare Academic Sciences Pvt Ltd. This is an open-access article under the CC BY license (<https://creativecommons.org/licenses/by/4.0/>) DOI: <https://dx.doi.org/10.22159/ijap.2022v14i2.43491>. Journal homepage: <https://innovareacademics.in/journals/index.php/ijap>

### INTRODUCTION

5-Fluorouracil (5-FU) is a cytotoxic drug used for treating colorectal, stomach, breast, and pancreatic cancer. It has been widely used in the treatment of cancer and it also exhibits an antibacterial activity [1]. Upon intravenous administration, it may cause severe side and toxic effects on the gastrointestinal tract, cardiac, neural and, transdermal system [2-4].

It is rapidly eliminated after intravenous injection with a half-life of 20 min [5, 6].

5-FU requires an effective delivery system for proper therapy; solid lipid nanoparticles (SLNs) have emerged as a promising system for delivering anti-cancer drugs. SLNs combine the advantages and avoid disadvantages of polymeric nanoparticles, fat emulsions, and liposomes.

Solid matrices in SLNs provide controlled release of drugs, thereby avoiding the burst release generally associated with fat emulsions [7].

SLNs have been used as drug carriers due to their cost-effectiveness and their suitable size. Anticancer drug-loaded SLNs were composed to decrease the cytotoxicity and increase the bioavailability of the anti-cancer drug [8].

SLNs improve the oral bioavailability of the drug through enhancing its transport from gut wall to systemic circulation, with a size range from (50-1000 nm) composed of physiological lipid, and at room temperature, particles are at solid state [9].

The use of nanoparticles as a 5-fluorouracil transporter reduced the viability of A549 cells (adenocarcinoma human alveolar basal epithelial cells) to a greater extent than the drug alone. This was

mainly due to the increased apoptosis, necrosis, and cell cycle arrest [10].

The drug-excipient compatibility study is a significant step in the pre-formulation phase for composing all forms of dosages. Physical and chemical interactions between drugs and excipients can influence the drug's stability, bioavailability, safety, and therapeutic efficacy [11].

Differential scanning calorimetry (DSC) provides information about the possible interactions between drug and excipient mixtures through thermal behavior and the appearance or disappearance of endothermic or exothermic peaks. If a drug is dispersed as a solid-solution state or molecular dispersion in the lipid system, there will not be any endotherm peak detected [12].

X-ray diffraction (XRD) and Fourier transform infrared spectroscopy (FT-IR) are complementary techniques confirming findings or possible functional group interactions [13].

In our research, the pre-formulation study of 5-FU with four different lipids was evaluated.

Cholesterol, Compritol®, stearic acid, and glycerol monostearate (GMS) are commonly used for developing solid lipid nanoparticles (SLNs).

Cholesterol is an essential component in the animal cell membrane [11]. It is used for preparing liposomes for drug delivery. It provides further rigidity to the membrane lipid bilayer, thus improving the liposome stability.

Compritol® is a lubricating agent in the production of an oral tablet [12]. It is used for formulating sustained-release tablets [13].

Stearic acid is a fatty acid found in animals and some fungi with a long chain consisting of 18 carbon atoms. It is also used for the preparation of SLNs [14].

GMS is used as an emulsifying agent in food, pharmaceuticals, and cosmetics [15]; monoglycerides are typically obtained from the glycolysis or hydrolysis of triglycerides or the direct esterification of glycerol with fatty acids [16].

For this purpose, DSC measurements were performed on 5-FU in pure form, 5-FU-physical mixtures with four lipids, and 5-FU blended mixtures with four lipids. Melting temperature peaks ( $T_m$ ) were compared with all measurements.

FT-IR and XRD were also used for compatibility study between 5-FU and lipids by checking shifts of functional groups of drug and crystalline state of the drug.

## MATERIALS AND METHODS

### Materials

5-FU was obtained from Hikma Pharmaceuticals (lot: fl41507602), Cairo, Egypt. Cholesterol was obtained from Pallav Chemicals, Boisar, India. Compritol® was obtained from Gattefosse, France. Stearic acid and dimethylsulfoxide were obtained from Al-Gomhorya Company, Cairo, Egypt. GMS was obtained from Central Drug House Company (New Delhi, India).

### Methods

#### Preparation of 5-FU-lipid physical mixtures

The physical mixture was made by mixing in a mortar with a pestle for 5 min. Four milligrams of drug with the same amount of lipid were mixed and stored in closed glass containers away from light and humidity (maintained in a refrigerator) for 24 h to be used for analysis [17].

The physical mixture was prepared by direct mixing (1:1) mass ratio in glass mortar to ensure homogenous mixing [18].

#### Preparation of 5-FU-lipid blended mixtures

Drug-lipid blended mixture was prepared by the simple solvent evaporation casting method [17].

The free drug solution was prepared by dissolving (160 mg) in dimethylsulfoxide (2 ml). The four lipids solutions (stearic acid, compritol®, GMS, and cholesterol) were melted at 60 °C.

The prepared solutions (drug and melted lipids) were poured into glass agar dishes and dried at room temperature for 48 h [18]. The residue after dryness was scratched by a spatula to conduct the consequent analysis.

#### DSC thermal analysis

Differential Scanning Calorimeter (DSC) (Perkin Elmer, Germany) equipped with an intercooler used for analysis. The enthalpy scale was done on the drug alone, physical mixtures, and blended mixtures. DSC was made on the 5-FU-lipid physical mixture (50% w/w), 5-FU-lipid (50% w/w) blended mixtures.

Appearance or disappearance of the drug melting peak may indicate an interaction between drug and excipients [19, 20].

Flat bottomed aluminum pans were sealed and heated under temperature from 30 °C to 450 °C with advanced computer software programs at a scanning rate of 10 min<sup>-1</sup> and thermograms were obtained [21].

#### XRD crystallography

Powdered samples (drug alone, 50% w/w drug-lipid ratio in the physical mixture) or 4 mg of each blended mixture (50% w/w drug-lipid ratio in the blended mixture) were exposed to monochromatic nickel-filtered copper radiation (40 kilovolts, 35 milliamperes) using Philips XRD equipment model PW/1710. The scanning range of 2θ angles was made under 2-60 °C at an angular speed of 0.03° per second [22].

### FT-IR spectral analysis

Infrared spectra of the drug, physical mixture and blended mixtures at functional group region (4000-400 cm<sup>-1</sup>) were measured. Powdered samples were analyzed by FT-IR spectrometer (Shimadzu, Tokyo, Japan). For analysis, discs were prepared by mixing the sample with a small amount of KBr and compressing the high-pressure mixture [22].

The powder samples (physical mixture or blended mixture) were gently mixed with 300 mg of potassium bromide powder compressed into discs at a force using a manual tablet presser. A 16 scan interferogram was collected for each spectrum with 4 cm<sup>-1</sup> resolution to the mid-IR region at room temperature. All samples were taken in triplicate and the data presented were the average of the three measurements [17].

## RESULTS AND DISCUSSION

### Thermal behavior, XRD and FTIR of 5-FU, and lipids

The thermogram of 5-FU (fig. 1) showed a characteristic sharp peak of pure 5-FU around 280.04 °C, mainly related to 5-FU melting point temperature ( $T_m$ ) [23, 24].

Peak around 148.58°C in the thermogram of cholesterol as shown in fig. 2(a) was related to the melting point of this lipid [25]. Then a sharp peak at 356.40°C was related to the decomposition temperature of lipid [26]. This melting point ensured the crystalline structure of this lipid. This result was confirmed by Rostamkalaei *et al.* [27].

Compritol® showed a peak around 72.68°C, which is the melting temperature of lipid [21, 27], while the peak at 330°C may be attributed to decomposition temperature ( $T_d$ ) as shown in fig. 2(b) [28].

The thermogram of stearic acid showed an endothermic peak at 53.13°C as presented in fig. 2(c) due to its melting point [29, 30].

An endothermic peak appeared at 65.2 °C in the thermogram of GMS as shown in fig. 2(d) indicating its melting point [29]. This sharp endothermic peak indicated the crystalline structure of GMS and confirmed the XRD result [31].

The XRD pattern of pure 5-FU had numerous sharp peaks at 2θ angles of 18.5110°, 20.5291°, 22.8284°, 27.1278° and 30.8148° as shown in fig. 3 indicating the crystalline state of the drug [32, 33].

Numerous peaks also appeared in the XRD pattern of pure cholesterol, indicating this lipid's crystalline structure [26, 27]. It showed peaks at 2θ angle 5.272°, 10.604°, 12.83°, 15.501°, 16.972°, 17.393°, 18.154°, 23.565°, 26.244°, 37.151°, and 42.404° as shown in fig. 4(a).

Compritol® as shown in fig. 4(b) showed peaks at a 2θ angle of 21.2033° and 23.6930° confirming its crystallinity [21]. The same result was approved by Rostamkalaei *et al.*, with sharp peaks obtained at 2θ angles of 21.16° and 25.48° [27].

XRD pattern of pure stearic acid as presented in fig. 4(c) showed peaks at 2θ angle of 20° and 24° [34]. The same result was obtained by Fang *et al.* [30].

The XRD pattern of pure GMS showed peaks at 2θ angles of 13°, 17°, 22°, and 24° as shown in fig. 4(d) confirming that GMS is crystalline [34]. The same finding was observed by Jia *et al.* [35].

FT-IR spectrum of pure 5-FU as presented in fig. 5 and table 1 showed peaks at 3136.25 cm<sup>-1</sup> due to N-H stretching, C=O stretching at 1658.78 cm<sup>-1</sup>, C=C stretching at 1446.61 cm<sup>-1</sup>, C-F stretching at 1431.18 cm<sup>-1</sup>, C-N stretching at 1246.02 cm<sup>-1</sup> and vibration of the pyrimidine ring at 1350.17 cm<sup>-1</sup> [32, 36].

FT-IR spectrum of cholesterol as shown in fig. 6(a) had bands at 3420 cm<sup>-1</sup> due to the presence of a water group and the hydroxyl group attached to the cholesterol ring. The bands were observed at the 2193-2931 cm<sup>-1</sup> referred to C-H stretching modes of aromatic compounds. C=O stretching was observed at 1651 cm<sup>-1</sup> and 1507 cm<sup>-1</sup>. C-H deformation band was observed at 1457 cm<sup>-1</sup>. Both CH<sub>2</sub> and CH<sub>3</sub> groups were at 1384 cm<sup>-1</sup>, owing to hydrogen bonding vibrations. The bands C-H were observed at 1149 cm<sup>-1</sup>. C-C-C bands

were observed at 1113 cm<sup>-1</sup>. The ring deformation of cholesterol can be assigned at 1050 cm<sup>-1</sup>.

Ring breathing was observed at 953 cm<sup>-1</sup> and C-C Stretching was observed at 853 cm<sup>-1</sup>. Ring deformation was observed at 701 cm<sup>-1</sup>, while the C-OH band was at 568 cm<sup>-1</sup> [37]. The major bands for cholesterol molecule were found between 2800–3000 cm<sup>-1</sup> due to asymmetric and symmetric stretching vibrations of CH<sub>2</sub> and CH<sub>3</sub> groups. The characteristic peak at 2899 cm<sup>-1</sup> was due to CH<sub>2</sub> symmetric stretching vibration, one double band (C = C) of cholesterol ring was at 1674 cm<sup>-1</sup> [38].

FT-IR spectrum of Compritol® as presented in fig. 6(b) showed absorption bands of C-H stretching at 2815 cm<sup>-1</sup>, 2849 cm<sup>-1</sup>, and C=O stretching at 1738 cm<sup>-1</sup> [21, 27].

FT-IR spectrum of stearic acid as presented in fig. 6(c) showed peaks at 2915 cm<sup>-1</sup>, 2945 cm<sup>-1</sup>, and 2847 cm<sup>-1</sup> indicating CH<sub>2</sub> stretching vibrations. The peaks at 1697.6 cm<sup>-1</sup> and 1430.0 cm<sup>-1</sup> were due to C=O (from carboxyl group) and O-H (hydroxyl group) band stretching, respectively. The symmetric stretching peaks of the carboxylic group COO appeared at 1410.5 cm<sup>-1</sup> and the anti-symmetric COO appeared at 1518 cm<sup>-1</sup>. The CH<sub>2</sub> fluctuating vibrations were seen in 1150-1350 cm<sup>-1</sup> due to stretching peaks of the carboxylic group [29, 30].

FT-IR spectrum of GMS showed peaks at three positions, including 2915 cm<sup>-1</sup>, 2955.3 cm<sup>-1</sup>, and 2848.5 cm<sup>-1</sup>, due to CH<sub>2</sub> stretching vibrations as presented in fig. 6(d). The carboxyl group (C=O) stretching peak was observed at 1729.6 cm<sup>-1</sup> [29].

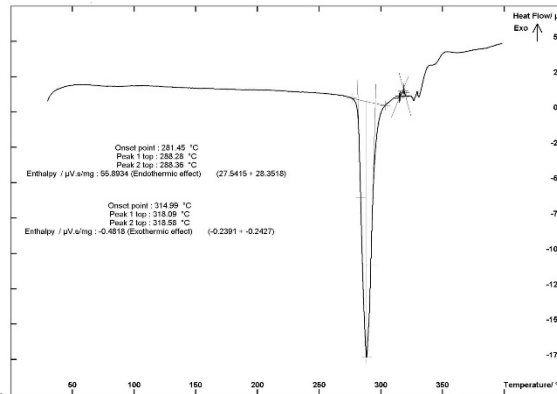


Fig. 1: DSC of pure 5-FU

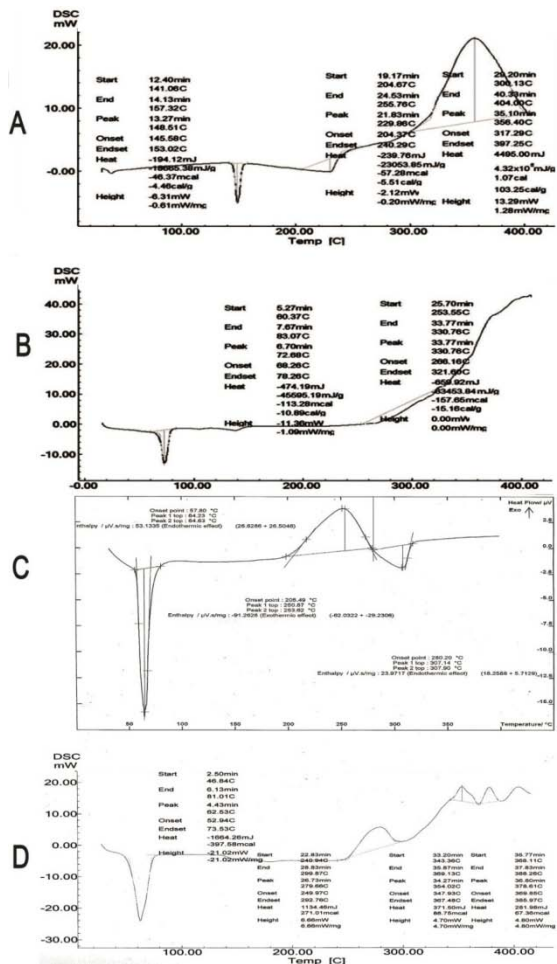


Fig. 2: DSC of: (A) Cholesterol (B) compritol® (C) Stearic acid (D) GMS

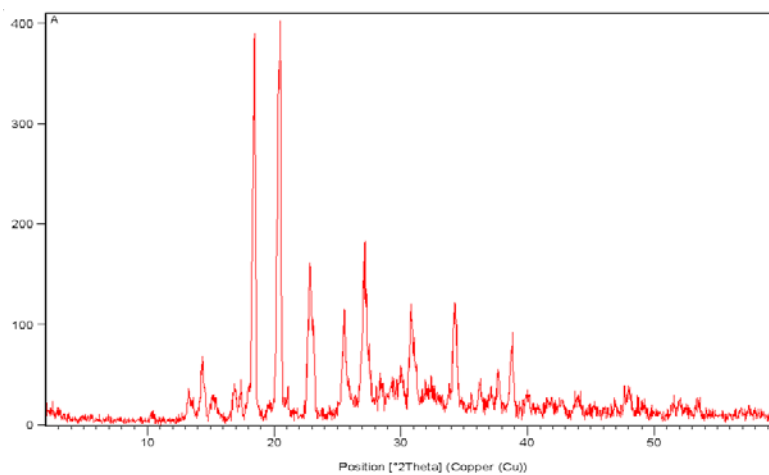


Fig. 3: XRD of pure 5-FU

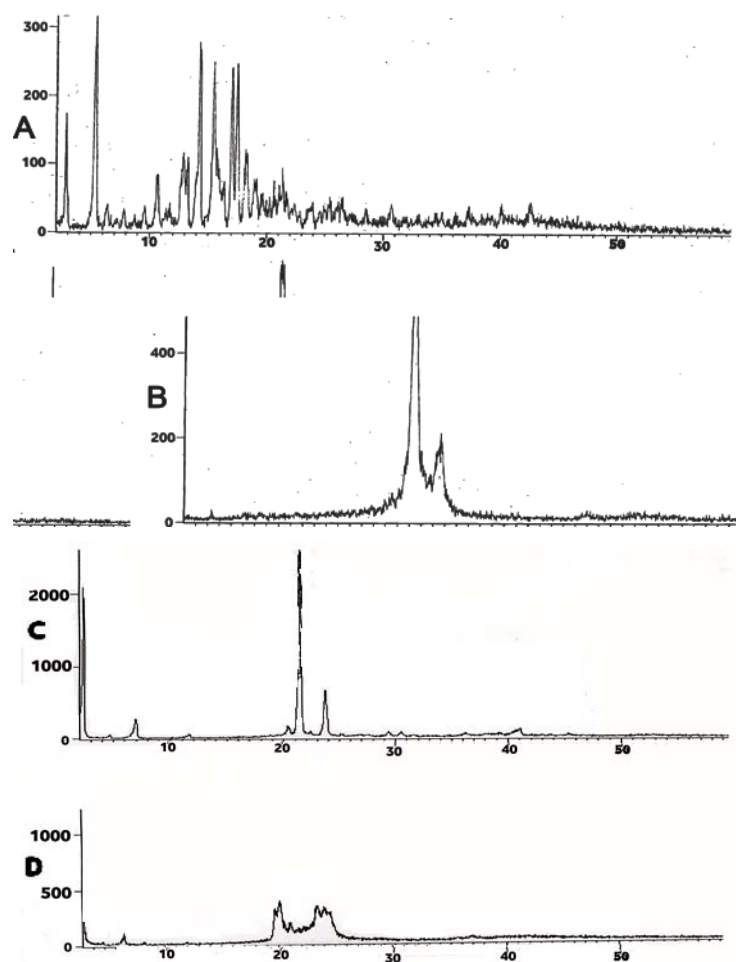


Fig. 4: XRD of: (A) Cholesterol (B) compritol®(C) Stearic acid (D) GMS

Table 1: FTIR bands of 5-FU (4000-400  $\text{cm}^{-1}$ )

Main function groups	Assignment	Wavenumber ( $\text{cm}^{-1}$ )
N-H	N-H stretching	3136.25 $\text{cm}^{-1}$
C=O	C=O bending	1658.78 $\text{cm}^{-1}$
C=C	C=C stretching	1500 $\text{cm}^{-1}$
C-F	C-F stretching	1431.18 $\text{cm}^{-1}$
C-N	C-N stretching	1246.02 $\text{cm}^{-1}$
Pyrimidine group	pyrimidine bending	1350.17 $\text{cm}^{-1}$

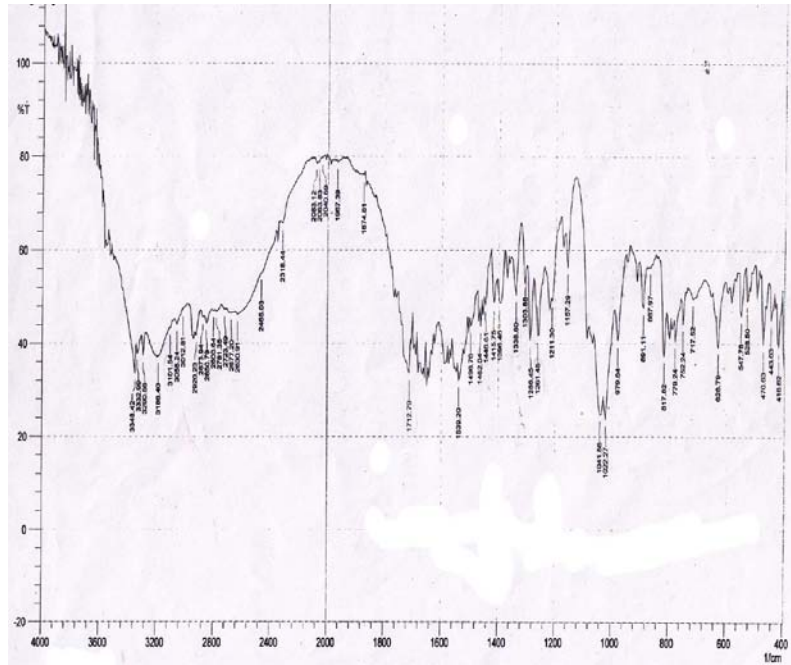


Fig. 5: The FTIR spectra of pure 5-FU

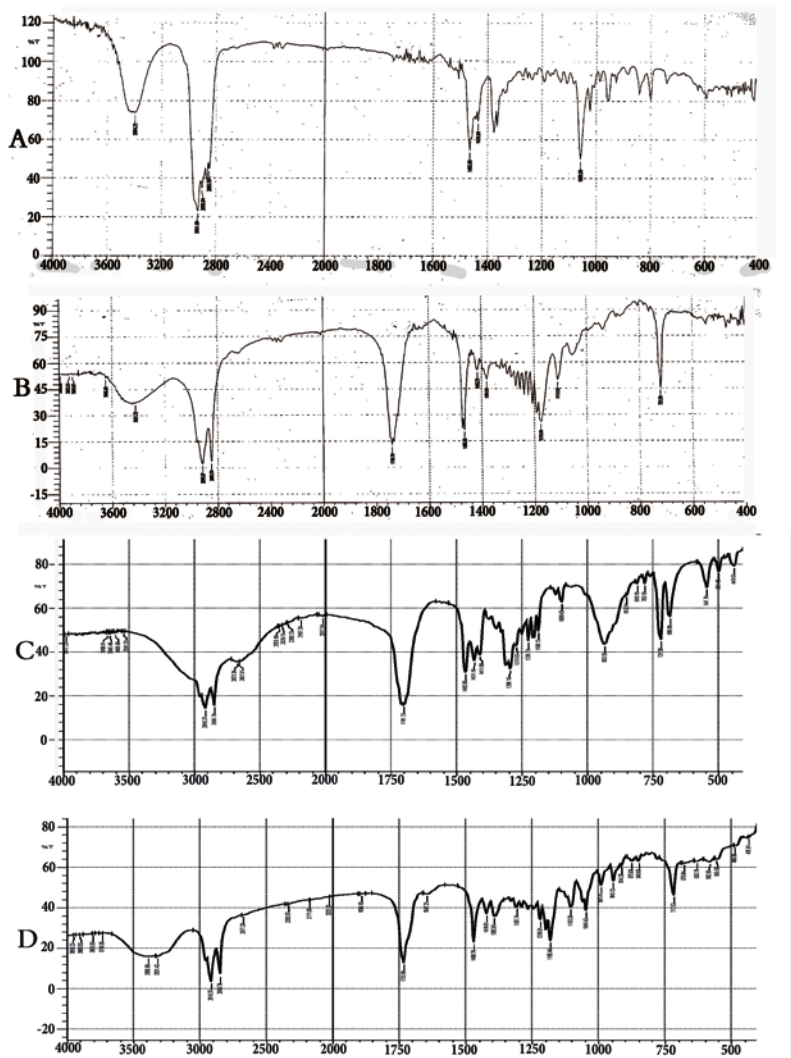


Fig. 6: FTIR of: (A) Cholesterol (B) compritol®(C) Stearic acid (D) GMS

### Pre-formulation studies with excipients

Thermal curves were used to detect any physical interactions between the drug and four lipids, consequently, chose the most proper lipid [19, 39]. 5-FU Tm (280.04 °C) peak appeared in all drug-physical mixtures with minor changes in position as shown in fig. 7 and table 2.

These results were similar to Gardouh *et al.*, at which a characteristic peak of the drug (Triamcinolone) was present in its physical mixture with GMS [40].

Regarding DSC results of 5-FU blended mixtures with lipids as shown in fig. 8 and table 3, it was clear that 5-FU Tm (280.04 °C) peak appeared in all drug-lipid blended mixtures with small changes excluding drug-cholesterol and drug-compritol® blended mixtures. 5-FU peak minor shifted in the drug-cholesterol blended mixture to (270.6 °C).

With cholesterol, as shown in fig. 8(a) and table 3 crystal form was changed, leading to the disappearance of endothermic peak of lipid and disappearance of melting peak of the drug indicated that drug was dispersed inside lipid matrix [41].

5-FU peak also shifted in the drug-Compritol® blended mixture to (238.47 °C) as shown in fig. 8(b) and table 3. Compritol® is partial glycerides with 15% monoglycerides and 50% diglycerides. The presence of these partial glycerides facilitate emulsification and form more rigid surfactant films [42]. Thus, leading to drug dispersion inside the matrix lipid and broadening of 5-FU melting peak. It was impossible to detect the separated melting peaks for compritol because of its complex structure during the heating scans due to its polymorphic nature [43]. When 5-FU was added to melted lipid, the drug was molecularly dispersed inside this lipid [44, 45] leading to the presence of amorphous drug state [44, 46-47]. The hydrogen bond may be formed between the fluorine atom of 5-FU and the hydroxyl group of cholesterol [48].

5-FU peak minor shifted in the drug-stearic acid blended mixture to (277.65 °C) as shown in fig. 8(c) and table 3 and not changed in GMS-blended mixture (280.84 °C) as depicted in fig. 8(d) and table 3.

Dehydration peaks appeared in the physical mixtures and blended mixtures at the range of 53 °C-113 °C may be due to the melting of the lipids [19]. The dehydration peak was small and appeared due to the lack of water absorption [28]. As for DSC, the heat given off during the reaction was called an exothermic reaction, while the heat absorbed by the material is called an endothermic reaction. By measuring the exothermic and endothermic reactions, it is possible to determine all the chemical and physical state changes in the sample [28].

The DSC was conducted to check the moisture content and volatile component present in samples [28].

XRD has been used for the identification of the crystalline state of 5-FU and the possible interaction of the drug with four lipids [49, 50]. XRD peak depends on crystal size because the crystalline nature of the drug was detected at a certain value at the 2θ range [51].

XRD of 5-FU-cholesterol physical mixture showed peaks at 2θ angle of 18.4°, 20.49°, 22.77°, 27.15°, and 30.7° as shown in fig. 9(a) and table 4. So; 5-FU was still in its crystalline state

XRD of 5-FU-compritol physical mixture showed drug peaks at 2θ angle of 18.39°, 20.44°, 22.68°, 27.20° and 30.72° as presented in fig. 9(b) and table 4. So; the crystalline state of the drug was maintained.

XRD of the 5-FU-stearic acid physical mixture showed drug peaks at 2θ angle of 16.43°, 20.7°, 22.87°, 27.10° and 30.88° as depicted in fig. 9(c) and table 4. So; distinct peaks of the drug were present.

XRD of 5-FU-GMS physical mixture showed drug peaks at 2θ angle of 19.25°, 20.86°, 21.98°, 28.74° and 32.28° as shown in fig. 9(d) and table 4. So; the crystalline state of the drug was still present.

5-FU peaks remained distinct in all physical mixtures of the drug with four lipids and the crystalline structure of the drug has been maintained [52]. Jia *et al.* confirmed this result when using GMS to

prepare silybin SLNs at which drug sharp peaks were still present in the physical mixture with lipid. In contrast, the degree of crystallinity of lipid is decreased when the drug is incorporated in SLNs [35].

The XRD of 5-FU-cholesterol blended mixture showed distinct peaks of the drug at 2θ angle of 19.04°, 20.7°, 21.8°, 28.59° and 31.01° as shown in fig. 10(a) and table 5, so crystallinity of drug was still present.

In the case of the 5-FU-compritol® blended mixture, numerous distinct peaks were disappeared while other peaks appeared in low intensities as shown in fig. 10(b) and table 5 indicating that the drug was in its amorphous state [44].

A slight decrease of intensity of peak, which is different from that of the pure drug was an indicator that the drug was molecularly dispersed inside lipid [51]. A similar finding was reported by Eleraky *et al.*, the reduced crystalline structure of the drug was observed for temazepam due to drug solubility in the lipid [53].

The XRD of the 5-FU-stearic acid blended mixture had distinct peaks of the drug at 2θ angle of 18.86°, 20.388°, 23.57°, 26.8°, and 30.65° as shown in fig. 10(c) and table 5 indicating the crystallinity of drug.

The XRD of 5-FU-GMS blended mixture showed distinct peaks of the drug at 2θ angle of 19.68°, 20.469°, 23.24°, 28.52° and 31.97° as shown in fig. 10(d) and table 5 indicating that the crystalline state of the drug was maintained.

FT-IR spectroscopy was used to examine the chemical interaction between 5-FU and lipids. It is a non-destructive method and is commonly used in the analysis of pharmaceutical powders. Any change of characteristic bands of drug or disappearance of these bands indicates interactions between drug and excipients [54, 55].

FT-IR analysis studies were performed on 5-FU alone, 5-FU-lipid physical mixtures (50% w/w), and 5-FU-lipid (50% w/w) blended mixtures.

The FT-IR spectrum of the physical mixture of 5-FU with four lipids showed that all characteristic peaks of the drug appeared with minor changes in its physical mixture with four lipids as presented in fig. 11 and table 6.

Concerning 5-FU-cholesterol physical mixture as shown in fig. 11(a) and table 6, there was a minor shift in the drug principal peaks at 3101 cm<sup>-1</sup>, 1658 cm<sup>-1</sup>, 1465 cm<sup>-1</sup>, 1442 cm<sup>-1</sup>, 1257 cm<sup>-1</sup> and 1338 cm<sup>-1</sup> for N-H stretching, C=O bending, C=C stretching, C-F stretching, C-N stretching and pyrimidine bending, respectively. A similar finding was confirmed by Katharotiya *et al.* [56].

In the case of the 5-FU-compritol® physical mixture, characteristic peaks of the drug at 3136 cm<sup>-1</sup>, 1640 cm<sup>-1</sup> and 1273 cm<sup>-1</sup> were also present, compritol® peaks at 2922 cm<sup>-1</sup>, 1707 cm<sup>-1</sup>, and 1592 cm<sup>-1</sup> were present as shown in fig. 11(b) and table 6 [57].

5-FU-stearic acid physical mixture showed characteristic peaks of drug with a minor shift at 3120 cm<sup>-1</sup>, 1685 cm<sup>-1</sup>, 1473 cm<sup>-1</sup>, 1431 cm<sup>-1</sup>, 1246 cm<sup>-1</sup> and 1346 cm<sup>-1</sup> for N-H stretching, C=O bending, C=C stretching, C-F stretching, C-N stretching and pyrimidine bending respectively as shown in fig. 11(c) and table 6.

5-FU-GMS physical mixture showed characteristic peaks of drug with a minor shift at 3066 cm<sup>-1</sup>, 1658 cm<sup>-1</sup>, 1473 cm<sup>-1</sup>, 1419 cm<sup>-1</sup>, 1246 cm<sup>-1</sup> and 1381 cm<sup>-1</sup> for N-H stretching C=O bending C=C stretching, C-F stretching, C-N stretching and pyrimidine bending respectively as shown in fig. 11(d) and table 6. A similar result was obtained by Patel *et al.* [2].

The FT-IR spectrum of 5-FU blended mixtures with four lipids showed no chemical interaction between drug and cholesterol or compritol® or GMS as shown in fig. 12 and table 7.

Characteristic peaks of the drug were minor shifted in 5-FU-cholesterol blended mixture at 3070 cm<sup>-1</sup>, 1658 cm<sup>-1</sup>, 1465 cm<sup>-1</sup>, 1431 cm<sup>-1</sup>, 1246 cm<sup>-1</sup> and 1350 cm<sup>-1</sup> for N-H stretching, C=O bending, C=C stretching, C-F stretching, C-N stretching and pyrimidine bending respectively as presented in fig. 12(a) and table 7.

Characteristic peaks of 5-FU were also present in a drug-compritol® blended mixture with a minor shift at 3005 cm<sup>-1</sup>, 1651 cm<sup>-1</sup>, 1408 cm<sup>-1</sup>, 1438 cm<sup>-1</sup>, 1246 cm<sup>-1</sup> and 1315 cm<sup>-1</sup> for N-H stretching, C=O bending, C=C stretching, C-F stretching, C-N stretching and pyrimidine bending respectively as depicted in fig. 12(b) and table 7.

In the case of stearic acid-drug blended mixture, the N-H peak at 3136.25 cm<sup>-1</sup> is disappeared as shown in fig. 12(c) and table 7. This result may be due to the interaction between stearic acid and 5-FU which led to the salt formation or formation of amide ester [58].

Conjugation of 5-FU with stearic acid resulted in the absence of the N-H group, which is present in 5-FU [59] N-H group is shown in region 3136 cm<sup>-1</sup> [60]. A similar finding was confirmed by Sauraj *et al.*, and a new peak appeared at 1730 cm<sup>-1</sup> due to the stretching frequency of the CO group in the case of lipophilic 5-FU stearic acid prodrug [61].

The FT-IR spectrum of 5-FU blended mixture with GMS when compared to 5-FU alone, as shown in fig. 12(d) and table 7, no significant change occurred for characteristic bands of the drug, especially for C=O band and N-H band. This result is confirmed by Patel *et al.* [2].

Finally, GMS does not affect the physicochemical properties of the drug, whether in a physical mixture or a blended mixture and it is compatible with the drug.

Shenoy *et al.* found that the partition coefficient of 5-FU in cetyl palmitate then GMS was the highest among various lipids [62]. GMS is of more than 12-carbons chain length; fatty acid chains present in the lipids can improve uptake of SLNs by lymphatic transport. The SLNs are taken up through the gastrointestinal tract and transported via intestinal lymph directly into the systemic circulation, thus bypassing the liver first-pass metabolism [63].

Table 2: DSC results of 5-FU-lipid physical mixtures

Significant DSC values of (°C)	
Sample	T <sub>m</sub>
Pure 5-FU	280.04
(A) 5-FU-cholesterol	278.43
(B) 5-FU-compritol®	280.87
(C) 5-FU-stearic acid	280.63
(D) 5-FU-GMS	283.85

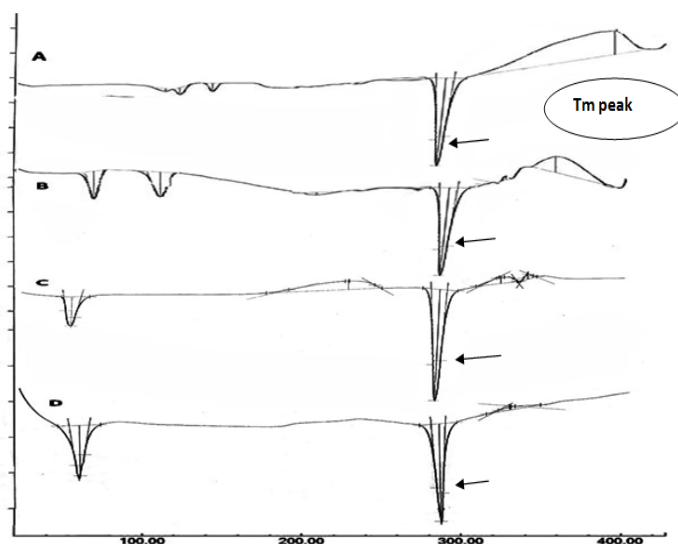


Fig. 7: DSC of (A) 5-FU-cholesterol physical mixture; (B) 5-FU-compritol® physical mixture; (C) 5-FU-stearic acid physical mixture; (D) 5-FU-GMS physical mixture

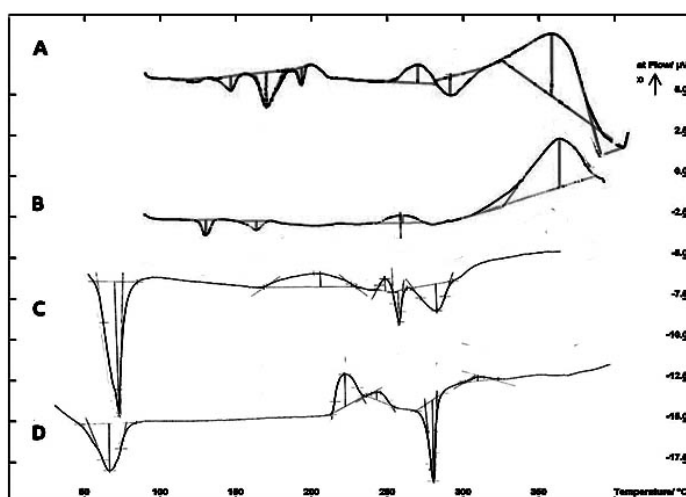
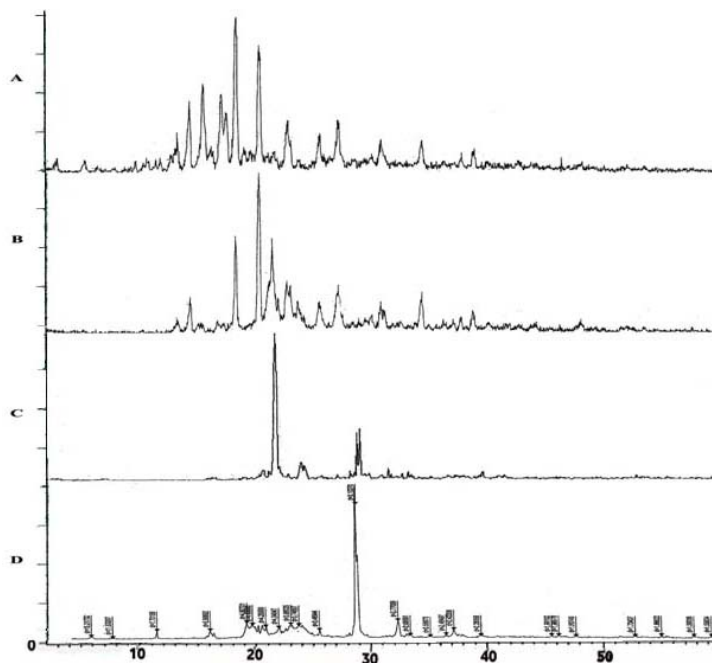


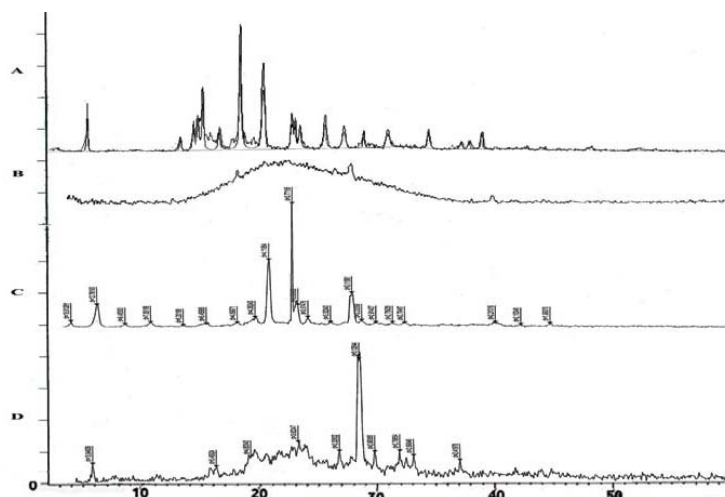
Fig. 8: DSC of (A) 5-FU-cholesterol blended mixture; (B) 5-FU-compritol® blended mixture; (C) 5-FU-stearic acid blended mixture; (D) 5-FU-GMS blended mixture

**Table 3: DSC results of 5-FU-lipid blended mixtures**

Significant DSC values of (°C)	
Sample	T <sub>m</sub>
Pure 5-FU	280.04
(A) 5-FU-cholesterol	270.61
(B) 5-FU-compritol®	238.47
(C) 5-FU-stearic acid	277.65
(D) 5-FU-GMS	280.84

**Fig. 9: XRD of (A) 5-FU-cholesterol physical mixture; (B) 5-FU-compritol® physical mixture; (C) 5-FU-stearic acid physical mixture; (D) 5-FU-GMS physical mixture****Table 4: XRD results of 5-FU-lipid physical mixtures**

Significant 2θ ° diffraction angle of						
Pure 5-FU	18.5	20.5	22.8	27.12	30.8	
(A) 5-FU-cholesterol	18.4	20.49	22.77	27.15	30.7	
(B) 5-FU-compritol®	18.39	20.44	22.68	27.20	30.72	
(C) 5-FU-stearic acid	16.43	20.70	22.87	27.10	30.88	
(D) 5-FU-GMS	19.25	20.86	21.98	28.74	32.28	

**Fig. 10: XRD of (A) 5-FU-cholesterol blended mixture; (B) 5-FU-compritol® blended mixture; (C) 5-FU-stearic acid blended mixture; (D) 5-FU-GMS blended mixture**

**Table 5: XRD results of 5-FU-lipid blended mixtures**

<b>Significant <math>^{\circ}2\theta</math> diffraction angle of:</b>						
Pure 5-FU	18.5	20.5	22.8	27.12	30.8	
(A) 5-FU-cholesterol	19.04	20.7	21.8	28.59	31.01	
(B) 5-FU-compritrol®	18.55	....	....	28.31	.....	
(C) 5-FU-stearic acid	18.86	20.388	23.57	26.8	30.65	
(D) 5-FU-GMS	19.68	20.469	23.24	28.52	31.97	

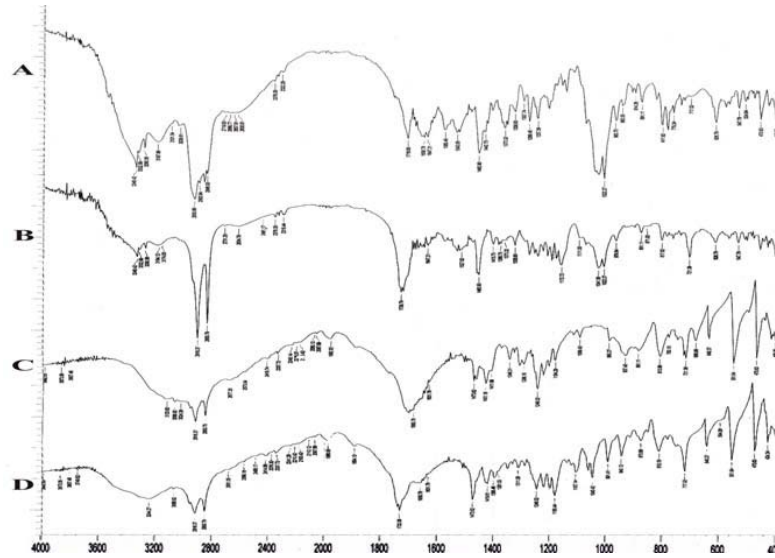


**Fig. 11: FTIR spectra of: (A) 5-FU-cholesterol physical mixture; (B) 5-FU-compritrol® physical mixture; (C) 5-FU-stearic acid physical mixture; (D) 5-FU-GMS physical mixture**

**Table 6: FTIR bands of 5-FU and its lipid physical mixtures (cm⁻¹)**

Main function groups	Assignment	5-FU	lipid-5-FU physical mixture			
			With cholesterol	With compritol®	With stearic acid	With GMS
N-H	N-H stretching	3136.25 cm⁻¹	3101.54 cm⁻¹	3174.83 cm⁻¹	3120.82 cm⁻¹	3066.82 cm⁻¹
C=O	C=O bending	1658.78 cm⁻¹	1658.78 cm⁻¹	1647.21 cm⁻¹	1685.79 cm⁻¹	1658.078 cm⁻¹
C=C	C=C stretching	1500.62 cm⁻¹	1465.9 cm⁻¹	1465.90 cm⁻¹	1473.62 cm⁻¹	1473.062 cm⁻¹
C-F	C-F stretching	1431.18 cm⁻¹	1442.75 cm⁻¹	1415.75 cm⁻¹	1431.18 cm⁻¹	1419.61 cm⁻¹
C-N	C-N stretching	1246.02 cm⁻¹	1257.59 cm⁻¹	1172.72 cm⁻¹	1246.02 cm⁻¹	1246.02 cm⁻¹
Pyrimidine group	pyrimidine bending	1350.17 cm⁻¹	1338.60 cm⁻¹	1338.6 cm⁻¹	1346.31 cm⁻¹	1381.03 cm⁻¹

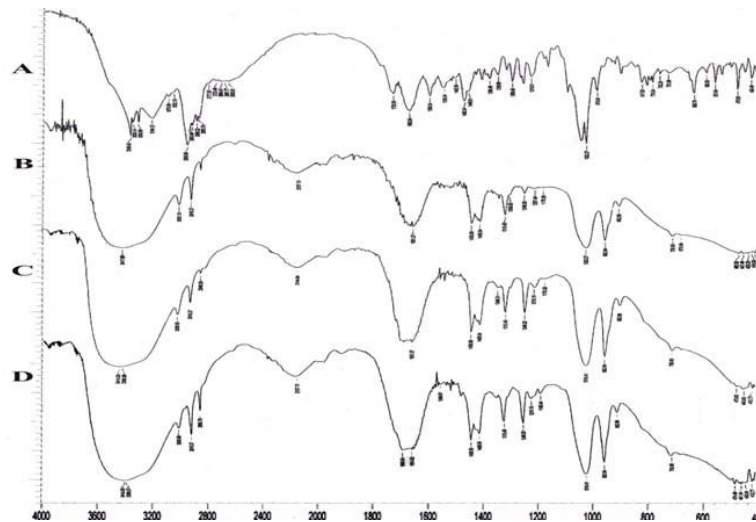


**Fig. 12: FTIR spectra of: (A) 5-FU-cholesterol blended mixture; (B) 5-FU-compritrol® blended mixture (C) 5-FU-stearic acid blended mixture (D) 5-FU-GMS blended mixture**

Table 7: FTIR bands of 5-FU and its lipid blends (cm<sup>-1</sup>)

Main function groups	Assignment	5-FU	lipid-5-FU blended mixtures			
			With cholesterol	With compritol®	With stearic acid	With GMS
N-H	N-H stretching	3136.25 cm <sup>-1</sup>	3070.60 cm <sup>-1</sup>	3005.10 cm <sup>-1</sup>	.....	3008.95 cm <sup>-1</sup>
C=O	C=O bending	1658.78 cm <sup>-1</sup>	1658.78 cm <sup>-1</sup>	1651.07 cm <sup>-1</sup>	1651.07 cm <sup>-1</sup>	1654.92 cm <sup>-1</sup>
C=C	C=C stretching	1500.62 cm <sup>-1</sup>	1465.90 cm <sup>-1</sup>	1408.04 cm <sup>-1</sup>	1438.90 cm <sup>-1</sup>	1546.91 cm <sup>-1</sup>
C-F	C-F stretching	1431.18 cm <sup>-1</sup>	1431.18 cm <sup>-1</sup>	1438.90 cm <sup>-1</sup>	1408.04 cm <sup>-1</sup>	1438.90 cm <sup>-1</sup>
C-N	C-N stretching	1246.02 cm <sup>-1</sup>	1246.02 cm <sup>-1</sup>	1246.02 cm <sup>-1</sup>	1246.02 cm <sup>-1</sup>	1246.02 cm <sup>-1</sup>
Pyrimidine group	pyrimidine bending	1350.17 cm <sup>-1</sup>	1350.17 cm <sup>-1</sup>	1315.45 cm <sup>-1</sup>	1346.31 cm <sup>-1</sup>	1315.45 cm <sup>-1</sup>

## CONCLUSION

The compatibility study of 5-FU with different four lipids (cholesterol, compritol®, stearic acid, GMS) was investigated by DSC analysis, XRD patterns, and FTIR. GMS and cholesterol were the most appropriate lipids with 5-FU.

DSC result showed that 5-FU peak (T<sub>m</sub>) (280 °C) was present in all physical mixtures and blended mixtures with the mentioned lipids except drug-compritol® blended mixture.

XRD results showed that 5-FU crystalline state was still found in all physical mixtures and blended mixtures with lipids except drug-compritol® blended mixture.

FTIR spectrum of physical mixtures and blended mixtures of 5-FU with mentioned lipids showed that all characteristic peaks of the drug appeared with minor changes in position, thus showing no significant physicochemical interaction. 5-FU-stearic acid blended mixture showed the absence of N-H peak of the drug at 3136.25 cm<sup>-1</sup>.

## ACKNOWLEDGMENT

The authors would like to acknowledge the help of the central lab, faculty of pharmacy, Cairo University, Cairo, Egypt.

## ETHICS APPROVAL

The study was performed according to ethics coded for experimental and clinical studies at the Faculty of Pharmacy, Cairo University (Cairo, Egypt), PI (1911).

## FUNDING

Nil

## AUTHORS CONTRIBUTIONS

All the authors have contributed equally.

## CONFLICTS OF INTERESTS

The authors declare no conflict of interest.

## REFERENCES

- Bakkialakshmi S, Chandrakala D. Thermodynamic studies on the interaction of 5-fluorouracil with human serum albumin. *Int J Pharm Pharm Sci.* 2012;5:46-9.
- Patel MN, Lakkadwala S, Majrad MS, Injeti ER, Gollmer SM, Shah ZA, Boddu SH, Nesamony J. Characterization and evaluation of 5-fluorouracil-loaded solid lipid nanoparticles prepared via a temperature-modulated solidification technique. *AAPS PharmSciTech.* 2014;15(6):1498-508. doi: 10.1208/s12249-014-0168-x, PMID 25035070.
- Smith T, Affram K, Nottingham EL, Han B, Amissah F, Krishnan S, Trevino J, Agyare E. Application of smart solid lipid nanoparticles to enhance the efficacy of 5-fluorouracil in the treatment of colorectal cancer. *Sci Rep.* 2020;10(1):16989. doi: 10.1038/s41598-020-73218-6, PMID 33046724.
- Wormann B, Bokemeyer C, Burmeister T, Köhne CH, Schwab M, Arnold D, Blohmer JU, Borner M, Brucker S, Cascorbi I, Decker T, de Wit M, Dietz A, Einsele H, Eisterer W, Folprecht G, Hilbe W, Hoffmann J, Knauf W, Kunzmann V, Largiadèr CR, Lorenzen S, Luftner D, Moehler M, Nöthen MM, Pox C, Reinacher-Schick A, Scharl A, Schlegelberger B, Seufferlein T, Sinn M, Stroth M, Tamm I, Trümper L, Wilhelm M, Wöll E, Hofheinz RD. Dihydropyrimidine dehydrogenase testing prior to treatment with 5-fluorouracil, capecitabine, and tegafur: A consensus paper. *Oncol Res Treat.* 2020;43(11):628-36. doi: 10.1159/000510258, PMID 33099551.
- Nasir B, Muhammad Ranjha N, Hanif M, Abbas G. Reverse-phase high-performance liquid chromatography method for determination of 5-fluorouracil in rabbit plasma. *Acta Pol Pharm.* 2017;74(2):379-83. PMID 29624242.
- Entezar Almahdi E, Mohammadi Samani S, Tayebi L, Farjadian F. Recent advances in designing 5-fluorouracil delivery systems: a stepping stone in the safe treatment of colorectal cancer. *Int J Nanomedicine.* 2020;15:5445-58. doi: 10.2147/IJN.S257700, PMID 32801699.
- Shenoy VS, Gude RP, Murthy RSR. *In vitro* anticancer evaluation of 5-fluorouracil lipid nanoparticles using B16F10 melanoma cell lines. *Int Nano Lett.* 2013;3(1):1-9.
- Bayat P, Pakravan P, Salouti M, Ezzati Nazhad Dolatabadi JEN. Lysine decorated solid lipid nanoparticles of epirubicin for cancer targeting and therapy. *Adv Pharm Bull.* 2021;11(1):96-103. doi: 10.34172/apb.2021.010, PMID 33747856.
- Begum MY, Gudipati PR. Formulation and evaluation of dasatinib-loaded solid lipid nanoparticles. *Int J Pharm Pharm Sci.* 2018;10(12):14-20. doi: 10.22159/ijpps.2018v10i12.27567.
- Wu DW, Huang CC, Chang SW, Chen TH, Lee H. Bcl-2 stabilization by paxillin confers 5-fluorouracil resistance in colorectal cancer. *Cell Death Differ.* 2015;22(5):779-89. doi: 10.1038/cdd.2014.170, PMID 25323586.
- Moura EA, Correia LP, Pinto MF, Procópio JVV, de Souza FS, Macedo RO. Thermal characterization of the solid-state and raw material fluconazole by thermal analysis and pyrolysis coupled to GC/MS. *J Therm Anal Calorim.* 2010;100(1):289-93. doi: 10.1007/s10973-009-0473-x.
- BH JG, Shankar S, Munisamy M, RS A, Sagar V. Development of pH-dependent chronomodulated delivery systems of 5-fluorouracil and oxaliplatin to treat colon cancer. *Int J Appl Pharm.* 2020;12(5):118-30.
- Bannach G, Cervini P, Cavalheiro ÉTG, Ionashiro M. Using thermal and spectroscopic data to investigate the thermal behavior of epinephrine. *Thermochim Acta.* 2010;499(1-2):123-7. doi: 10.1016/j.tca.2009.11.012.
- Kalepu S, Manthina M, Padavala V. Oral lipid-based drug delivery systems- an overview. *Acta Pharm Sin B.* 2013;3(6):361-72. doi: 10.1016/j.apsb.2013.10.001.
- Avery MA, Jennings White C, Chong WKM. Simplified analogs of the antimalarial artemisinin: synthesis of 6, 9-desmethylartemisinin. *J Org Chem.* 1989;54(8):1792-5. doi: 10.1021/jo00269a009.
- Sonntag NOV. Glycerolysis of Fats and methyl esters-status, review and critique. *J Am Oil Chem Soc.* 1982;59(10):795A-802A. doi: 10.1007/BF02634442.
- Mohamed Al, Samir M, El-Seidi EA, Hathout RMH, Abdel G, Awad S. Effect of certain pharmaceutical polymers on lomefloxacin activity against helicobacter pylori. *Journal of Pharmaceuticals* 2013;1(1):1-11.
- Rojas Oviedo I, Retchkiman Corona B, Quirino Barreda CT, Cardenas J, Schabes Retchkiman PS. Solubility enhancement of a poorly water-soluble drug by forming solid dispersions using mechanochemical activation. *Indian J Pharm Sci.* 2012;74(6):505-11. doi: 10.4103/0250-474X.110576, PMID 23798775.
- Tita B, Fulias A, Bandur G, Marian E, Tița D. Compatibility study between ketoprofen and pharmaceutical excipients used in

- solid dosage forms. *J Pharm Biomed Anal.* 2011;56(2):221-7. doi: 10.1016/j.jpba.2011.05.017, PMID 21665404.
20. Slobozeanu AE, Bejan SE, Tudor IA, Mocioiu AM, Motoc AM, Romero Sanchez MD, Botan M, Catalin CG, Madalina CL, Piticescu RR, Predescu C. A review on differential scanning calorimetry as a tool for thermal assessment of nanostructured coatings. *Manuf Rev.* 2021;8:1. doi: 10.1051/mfreview/2020038.
  21. Aburahma MH, Badr-Eldin SM. Compritol 888 ATO: a multifunctional lipid excipient in drug delivery systems and nanopharmaceuticals. *Expert Opin Drug Deliv.* 2014;11(12):1865-83. doi: 10.1517/17425247.2014.935335, PMID 25152197.
  22. Pignatello R, Ferro M, Puglisi G. Preparation of solid dispersions of nonsteroidal anti-inflammatory drugs with acrylic polymers and studies on mechanisms of drug-polymer interactions. *AAPS PharmSciTech.* 2002;3(2):E10. doi: 10.1208/pt030210, PMID 12916947.
  23. Olukman M, Sanlı O, Solak EK. Release of anticancer drug 5-fluorouracil from different ionically crosslinked alginate beads. *J Biomater Nanobiotechnology.* 2012;3(4):469-79. doi: 10.4236/jbnb.2012.34048.
  24. Mohammed AM, Osman SK, Saleh KI, Samy AM. *In vitro* release of 5-fluorouracil and methotrexate from different thermosensitive chitosan hydrogel systems. *AAPS PharmSciTech.* 2020;21(4):131. doi: 10.1208/s12249-020-01672-6, PMID 32405869.
  25. Moghimipour E, Handali S. Utilization of thin film method for preparation of celecoxib loaded liposomes. *Adv Pharm Bull.* 2012;2(1):93-8. doi: 10.5681/apb.2012.013, PMID 24312776.
  26. Vyas PM, Vasant SR, Hajiyani RR, Joshi MJ, editors. Synthesis and Characterization of cholesterol Nano particles by using w/o microemulsion Technique. *AIP Conf Proc;* 2010.
  27. Rostamkalaei SS, Akbari J, Saeedi M, Morteza Semnani K, Nokhodchi A. Topical gel of metformin solid lipid nanoparticles: A hopeful promise as a dermal delivery system. *Colloids Surf B Biointerfaces.* 2019;175:150-7. doi: 10.1016/j.colsurfb.2018.11.072, PMID 30530000.
  28. Chiang TC, Hamdan S, Osman MS. Urea-formaldehyde composites reinforced with Sago fibres analysis by FTIR, TGA, and DSC. *Adv Mater Sci Eng.* 2016;2016:1-10. doi: 10.1155/2016/5954636.
  29. Hussain T, Saeed T, Mumtaz AM, Javaid Z, Abbas K, Awais A, Idrees HA. Effect of two hydrophobic polymers on the release of gliclazide from their matrix tablets. *Acta Pol Pharm* 2013;70(4):749-57. PMID 23923399.
  30. Fang G, Li H, Chen Z, Liu X. Preparation and characterization of stearic acid/expanded graphite composites as thermal energy storage materials. *Energy.* 2010;35(12):4622-6. doi: 10.1016/j.energy.2010.09.046.
  31. Kang JH, Yoo KH, Park HY, Hyun SM, Han SD, Kim DW, Park CW. Preparation and *in vivo* evaluation of a lidocaine self-nanoemulsifying ointment with glycerol monostearate for local delivery. *Pharmaceutics.* 2021;13(9):1468. doi: 10.3390/pharmaceutics13091468, PMID 34575544.
  32. Reddy D. Formulation and *in vitro* evaluation of antineoplastic drug loaded nanoparticles as drug delivery system. *Afr J Pharm Pharmacol.* 2013;7(23):1592-604. doi: 10.5897/AJPP2013.3436.
  33. Fouladian P, Kohlhagen J, Arafat M, Afinjuomo F, Workman N, Abuhelwa AY, Song Y, Garg S, Blencowe A. Three-dimensional printed 5-fluorouracil eluting polyurethane stents for the treatment of oesophageal cancers. *Biomater Sci.* 2020;8(23):6625-36. doi: 10.1039/d0bm01355b, PMID 33057525.
  34. BA, DN, Veerabrahma K. Development of olmesartan medoxomil lipid-based nanoparticles and nanosuspension: preparation, characterization and comparative pharmacokinetic evaluation. *Artif Cells Nanomed Biotechnol.* 2018;46(1):126-37. doi: 10.1080/21691401.2017.1299160. PMID 28290712.
  35. Jia LJ, Zhang DR, Li ZY, Feng FF, Wang YC, Dai WT, Duan CX, Zhang Q. Preparation and characterization of silybin-loaded nanostructured lipid carriers. *Drug Deliv.* 2010;17(1):11-8. doi: 10.3109/10717540903431586, PMID 19941406.
  36. Yusefi M, Shamel K, Jahangirian H, Teow SY, Umakoshi H, Saleh B, Rafiee-Moghaddam R, Webster TJ. The potential anticancer activity of 5-fluorouracil loaded in cellulose fibers isolated from rice straw. *Int J Nanomedicine.* 2020;15:5417-32. doi: 10.2147/IJN.S250047, PMID 32801697.
  37. Vasuki G, Selvaraju R. Growth and thermal characterization of cholesterol crystals. *Int J Modn Res Rev.* 2014;2(9):287-9.
  38. Gupta U, Singh VK, Kumar V, Khajuria Y. Spectroscopic studies of cholesterol: fourier transform infra-red and vibrational frequency analysis. *Materials Focus.* 2014;3(3):211-7.
  39. Cisse A, Peters J, Lazzara G, Chiappisi L. PyDSC: a simple tool to treat differential scanning calorimetry data. *J Therm Anal Calorim.* 2021;145(2):403-9. doi: 10.1007/s10973-020-09775-9.
  40. Gardouh A. Design and characterization of glyceryl monostearate solid lipid nanoparticles prepared by high shear homogenization. *BJPR* 2013;3(3):326-46. doi: 10.9734/BJPR/2013/2770.
  41. Wang M, Yuan Y, Gao Y, Ma HM, Xu HT, Zhang XN, Pan WS. Preparation and characterization of 5-fluorouracil pH-sensitive niosome and its tumor-targeted evaluation: *in vitro* and *in vivo*. *Drug Dev Ind Pharm.* 2012;38(9):1134-41. doi: 10.3109/03639045.2011.641565, PMID 22182601.
  42. Jenning V, Thünemann AF, Gohla SH. Characterisation of a novel solid lipid nanoparticle carrier system based on binary mixtures of liquid and solid lipids. *Int J Pharm.* 2000;199(2):167-77. doi: 10.1016/s0378-5173(00)00378-1, PMID 10802410.
  43. Souto EB, Mehnert W, Müller RH. Polymorphic behaviour of compritol 888 ATO as bulk lipid and as SLN and NLC. *J Microencapsul.* 2006;23(4):417-33. doi: 10.1080/02652040600612439, PMID 16854817.
  44. Nasr M, Ghorab MK, Abdelazem A. *In vitro* and *in vivo* evaluation of cubosomes containing 5-fluorouracil for liver targeting. *Acta pharm sin B.* 2015;5(1):79-88. doi: 10.1016/j.apsb.2014.12.001, PMID 26579429.
  45. Fouad EA, Yassin AEB, Alajami HN. Characterization of celecoxib-loaded solid lipid nanoparticles formulated with tristearin and softisan 100. *Trop J Pharm Res.* 2015;14(2):205-10. doi: 10.4314/tjpr.v14i2.3.
  46. Maher S, Santos A, Kumeria T, Kaur G, Lambert M, Forward P, Evdokiou A, Losic D. Multifunctional microspherical magnetic and pH-responsive carriers for combination anticancer therapy engineered by droplet-based microfluidics. *J Mater Chem B.* 2017;5(22):4097-109. doi: 10.1039/c7tb00588a, PMID 32264142.
  47. Arafat M, Fouladian P, Wignall A, Song Y, Parikh A, Albrecht H, Prestidge CA, Garg S, Blencowe A. Development and *in vitro* evaluation of 5-fluorouracil-eluting stents for the treatment of colorectal cancer and cancer-related obstruction. *Pharmaceutics.* 2020;13(1):17. doi: 10.3390/pharmaceutics13010017, PMID 33374233.
  48. Andalib S, Varshosaz J, Hassanzadeh F, Sadeghi H. Optimization of LDL targeted nanostructured lipid carriers of 5-FU by a full factorial design. *Adv Biomed Res.* 2012;1:45. doi: 10.4103/2277-9175.100147, PMID 23326776.
  49. Stulzer HK, Rodrigues PO, Cardoso TM, Matos JSR, Silva MAS. Compatibility studies between captopril and pharmaceutical excipients used in tablets formulations. *J Therm Anal Calorim.* 2008;91(1):323-8. doi: 10.1007/s10973-006-7935-1.
  50. Rodriguez I, Gautam R, Tinoco AD. Using X-ray diffraction techniques for biomimetic drug development, formulation, and polymorphic characterization. *Biomimetics (Basel).* 2020;6(1):1. doi: 10.3390/biomimetics6010001, PMID 33396786.
  51. Tummala S, Satish Kumar MN, Prakash A. Formulation and characterization of 5-fluorouracil enteric-coated nanoparticles for sustained and localized release in treating colorectal cancer. *Saudi Pharm J.* 2015;23(3):308-14. doi: 10.1016/j.jsps.2014.11.010, PMID 26106279.
  52. Sekhar EC, Rao KK, Raju RR. Chitosan/guar gum-g-acrylamide semi IPN microspheres for controlled release studies of 5-fluorouracil. *J Appl Pharm Sci.* 2011;1(8):199.
  53. Eleraky EN, M Omar M, A Mahmoud H, A Abou Taleb H. Nanostructured lipid carriers to mediate brain delivery of temazepam: design and *in vivo* study. *Pharmaceutics.* 2020;12(5):451.

54. Freire FD, Aragao CFS, de Lima e Moura TFA, Raffin FN. Compatibility study between chlorpropamide and excipients in their physical mixtures. *J Therm Anal Calorim.* 2009;97(1):355-7. doi: 10.1007/s10973-009-0258-2.
55. Kelani KM, Rezk MR, Monir HH, ElSherbiny MS, Eid SM. FTIR combined with chemometric tools (fingerprinting spectroscopy) in comparison to HPLC: which strategy offers more opportunities as a green analytical chemistry technique for pharmaceutical analysis. *Anal Methods.* 2020;12(48):5893-907. doi: 10.1039/d0ay01749c, PMID 33290449.
56. Katharotiya K, Shinde G, Katharotiya D, Shelke S, Patel R, Kulkarni D, Panzade P. Development, evaluation and biodistribution of stealth liposomes of 5-fluorouracil for effective treatment of breast cancer. *J Liposome Res.* 2021;1-13. doi: 10.1080/08982104.2021.1905661, PMID 33847220.
57. Borderwala K, Rathod S, Yadav S, Vyas B, Shah P. Eudragit S-100 surface engineered nanostructured lipid carriers for colon targeting of 5-fluorouracil: optimization and *in vitro* and *in vivo* characterization. *AAPS PharmSciTech.* 2021;22(6):1-15216. doi: 10.1208/s12249-021-02099-3, PMID 34386888.
58. Butler RN, O'Regan CB, Moynihan P. Reactions of fatty acids with amines. Part 2. Sequential thermal reactions of stearic (octadecanoic) acid with some 1,2- and 1,3-aminoalcohols and bis-amines. *J Chemical Society, Perkin Transactions 1.* 1978;(4):373-7. doi: 10.1039/p19780000373.
59. Raman S. Formulation and *in vitro* characterization of 5-fluorouracil and flavonoid dual lipid drug conjugates loaded self nanomulsifying drug delivery system for cancer targeting. *IJPSR.* 2019;10(7).
60. Miri B, Motakef Kazemi N, Shojaosadati SA, Morsali A. Application of a nanoporous metal-organic framework based on iron carboxylate as drug delivery system. *Iran J Pharm Res.* 2018;17(4):1164-71. PMID 30568676.
61. Kumar V, Kumar B, Deeba F, Bano S, Kulshreshtha A, Gopinath P, Sauraj, Kumar V, Kumar B, Deeba F, Bano S, Kulshreshtha A, Gopinath P, Negi YS. Lipophilic 5-fluorouracil prodrug encapsulated xylan-stearic acid conjugates nanoparticles for colon cancer therapy. *International J Biological Macromolecules.* 2019;128:204-13. doi: 10.1016/j.ijbiomac.2019.01.101, PMID 30684574.
62. Shenoy VS, Gude RP, Murthy RSR. *In vitro* anticancer evaluation of 5-fluorouracil lipid nanoparticles using B16F10 melanoma cell lines. *Int Nano Lett.* 2013;3(1). doi: 10.1186/2228-5326-3-36.
63. Nirbhavane P, Vemuri N, Kumar N, Khuller GK. Lipid nanocarrier-mediated drug delivery system to enhance the oral bioavailability of rifabutin. *AAPS PharmSciTech.* 2017;18(3):829-37. doi: 10.1208/s12249-016-0559-2, PMID 27350276.